

# EXCLUSIVE NONLEPTONIC BOTTOM TO CHARM BARYON DECAYS INCLUDING NONFACTORIZABLE CONTRIBUTIONS

M. A. IVANOV<sup>1</sup>, J. G. KÖRNER<sup>2</sup>, V. E. LYUBOVITSKIJ<sup>1,3</sup> and A. G. RUSETSKY<sup>1,4</sup>

<sup>1</sup> *Bogoliubov Laboratory of Theoretical Physics, JINR,  
Dubna (Moscow region), 141980 Russia*

<sup>2</sup> *Johannes Gutenberg-Universität, Institut für Physik, D-55099 Mainz, Germany*

<sup>3</sup> *Department of Physics, Tomsk State University, 634050 Tomsk, Russia*

<sup>4</sup> *IHEP, Tbilisi State University, 380086 Tbilisi, Georgia*

Exclusive nonleptonic decays of bottom baryons to charm baryons and pseudoscalar light mesons are analyzed within a relativistic three-quark model. We include factorizing as well as nonfactorizing contributions to the decay amplitudes. The total contribution of the nonfactorizing diagrams amount up to 30 % of the factorizing contributions in amplitude. We present detailed predictions for rates and asymmetry parameters.

## 1. Introduction

Recently there has been much progress in the experimental analysis of decays of heavy baryons <sup>1-3</sup>. From a number of experimental collaborations (ALEPH, ARGUS, ACCMOR, CLEO, OPAL, etc.) there exist many results on the mass spectrum, lifetimes, branching ratios and asymmetry parameters of heavy baryon decays. In the near future one can expect large quantities of new data on exclusive nonleptonic bottom baryon decays which calls for a comprehensive theoretical analysis of these decays.

The analysis of nonleptonic heavy baryon decays is complicated by the necessity of having to include nonfactorizing contributions. One thus has to go beyond the factorization approximation which has proved quite useful in the analysis of the exclusive nonleptonic decays of heavy mesons <sup>4</sup>. There have been some theoretical attempts to analyze nonleptonic heavy baryon decays using the factorizing contributions alone <sup>5</sup>, the argument being that  $W$ -exchange contributions can be neglected in analogy to the power suppressed  $W$ -exchange contributions in the inclusive nonleptonic decays of heavy baryons. One might even be tempted to drop the nonfactorizing contributions on account of the fact that they are superficially proportional to  $1/N_c$ . However, since  $N_c$ -baryons contain  $N_c$  quarks an extra combinatorial factor proportional to  $N_c$  appears in the amplitudes which cancels the explicit diagrammatic  $1/N_c$  factor <sup>6,7</sup>. There is now ample empirical evidences in the  $c \rightarrow s$

sector that the nonfactorizing diagrams cannot be neglected. For example, the two observed decays  $\Lambda_c^+ \rightarrow \Xi^0 K^+$  and  $\Lambda_c^+ \rightarrow \Sigma \pi$  can only proceed via the nonfactorizing diagrams. Their sizeable observed branching ratios may thus serve to obtain a measure of the size of the nonfactorizing contributions.

In this paper we present a complete analysis of the exclusive nonleptonic decays of bottom baryons ( $\frac{1}{2}^+$ ) into charm baryons ( $\frac{1}{2}^+$ ) and light pseudoscalar mesons ( $0^-$ ) within the so-called *Lagrangian spectator model* which has been developed from relativistic quark model<sup>8-11</sup> and may be viewed as the generalization of the spectator quark model<sup>12</sup>. Both factorizing and nonfactorizing diagrams can be evaluated in a self-consistent manner within this approach. We calculate branching ratios and the asymmetry parameters of all the decays in this class. The main result of our analysis is that the nonfactorizing contributions are important also in the  $b \rightarrow c$  sector and cannot be neglected. In the decays with both factorizing and nonfactorizing contributions the nonfactorizing diagrams contribute destructively and can amount up to 30 % of the nonfactorizing contribution in amplitude. Some of the decay channels as e.g.  $\Lambda_b^0 \rightarrow \Sigma_c^+ \pi^-$  and  $\Xi_b^0 \rightarrow \Sigma_c^+ K^-$  have no factorizing contribution but are predicted to occur in our approach albeit with a small branching fraction. It would be important to have an experimental confirmation of this prediction.

## 2. Lagrangian spectator model

In this paper we will use a relativistic quark model developed in<sup>8,9</sup> to calculate nonleptonic decays of heavy baryons. This model has been successfully applied to the description of the electromagnetic properties of nucleons<sup>10</sup> and has been extended to an analysis of the semileptonic decays of heavy baryons<sup>11</sup>. Since the evaluation of the nonleptonic decay amplitudes involves three-loop diagrams with nonlocal vertices, we shall make some simplifying assumptions which, on the one hand, have a clear physics motivation, and, on the other hand, allow one to evaluate both the factorizing and the nonfactorizing contributions to nonleptonic baryon decays.

Let us begin by recalling some of the crucial points of the approach developed in<sup>8-11</sup>. We consider the hadron to be a bound state of relativistic constituent quarks. The coupling of the hadrons to their constituent quarks is described by an interaction Lagrangian with an effective vertex function characterizing the momentum distribution of the constituents.

The Lagrangian describing the interaction of baryons with the three-quark current is

written as

$$\begin{aligned} \mathcal{L}_B^{\text{int}}(x) &= g_B \bar{B}(x) \int dy_1 \int dy_2 \int dy_3 \delta \left( x - \frac{\sum_i m_i y_i}{\sum_i m_i} \right) F \left( \frac{\Lambda_B^2}{18} \sum_{i < j} (y_i - y_j)^2 \right) \\ &\times J_B(y_1, y_2, y_3) + \text{h.c.} \end{aligned} \quad (1)$$

where  $J_B(y_1, y_2, y_3) = \Gamma_1 q^{a_1}(y_1) q^{a_2}(y_2) C \Gamma_2 q^{a_3}(y_3) \varepsilon^{a_1 a_2 a_3}$  is the three-quark current with the quantum numbers of the baryon  $B$ . The spatial four-coordinates  $y_i$  ( $i=1,2,3$ ) of the quarks are expressed through the c.m. coordinate ( $x$ ) and the relative Jacobi coordinates  $(\xi_1, \xi_2)$ <sup>11</sup>. The  $\Gamma_{1,2}$  are strings of Dirac matrices,  $C$  is the charge conjugation matrix, and  $a_i$  are colour indices.

The spin-flavour structure of heavy-light baryon currents has been studied in detail in the papers<sup>11,13,14</sup>. It was shown that in the heavy quark limit there are two currents for  $\Lambda$ -type baryons containing a light diquark with spin zero and two currents for  $\Omega$ -type baryons having a light diquark with spin 1. In ref.<sup>11</sup> we have shown that in the heavy quark limit the heavy quark factorizes from the light degrees of freedom. Then the Lagrangian which describes the interaction of  $\Lambda_Q$ -baryon with the constituent quarks may be written as

$$\begin{aligned} \mathcal{L}_{\Lambda_Q}^{\text{int}}(x) &= g_{\Lambda_Q} \bar{\Lambda}_Q(x) \Gamma_1 Q^a(x) \int d\xi_1 \int d\xi_2 F(\Lambda_{B_Q}^2 \cdot [\xi_1^2 + \xi_2^2]) \\ &\times u^b(x + 3\xi_1 - \xi_2 \sqrt{3}) C \Gamma_2 d^c(x + 3\xi_1 + \xi_2 \sqrt{3}) \varepsilon^{abc} + \text{h.c.} \end{aligned} \quad (2)$$

where  $\Gamma_1 \otimes C \Gamma_2 = I \otimes C \gamma^5$  or  $\gamma_\mu \otimes C \gamma^\mu \gamma^5$ . The explicit form of the interaction Lagrangians of light baryons with their constituents can be found in Ref.<sup>11</sup>.

We are modelling the effective vertex function  $F$  in Eq. (1) by the Gaussian shape factor  $F(k_E^2) = \exp(-k_E^2/\Lambda_B^2)$  which falls off sufficiently fast in the Euclidean region to provide for the ultraviolet convergence of the matrix elements. It was shown in<sup>11</sup> that the requirement of the correct unit normalization of the baryonic IW-functions  $\zeta(\omega)$  and  $\xi_1(\omega)$  at zero recoil  $\omega = 1$  imposes the condition  $\Lambda_{B_b} = \Lambda_{B_c}$ . For light baryons we introduce the cutoff parameter  $\Lambda_{B_q}$ . The cutoff parameters  $\Lambda_{B_Q} = \Lambda_{B_b} = \Lambda_{B_c}$  and  $\Lambda_{B_q}$  are the adjustable parameters.

The Lagrangian spectator model has been derived from the relativistic quark model<sup>8-11</sup>. It aims to reproduce the spin amplitude structure of the spectator (or static quark) model analysis<sup>6</sup>. This can be achieved by assigning the projector  $V_+ = (1 + \not{p})/2$  to each light quark field in the baryon-quark vertex, and by using the static approximation for  $u$ ,  $d$  and  $s$  quark propagators

$$\langle 0 | T \{ q(x) \bar{q}(y) \} | 0 \rangle = \frac{1}{\Lambda_q} \delta^{(4)}(x - y) \quad (3)$$

where  $\Lambda_q$  is the free parameter having the dimension of mass. We choose this parameter to have the same value  $\Lambda$  for  $u$  and  $d$  quarks and a different value  $\Lambda_s$  for the strange quark. Note that in this model the above two options of pseudoscalar and axial currents for the  $\Lambda$ -type baryon and two options of vector and tensor currents for the  $\Omega$ -type baryon become equivalent in the Lagrangian spectator model. It may be seen by using the equation of motion  $\bar{B}_Q(x) \not{v} = \bar{B}_Q(x)$ . The baryon-quark coupling constants in Eqs.(1,2) are fixed from *the compositeness condition* which is equivalent to the unit normalization of the elastic baryon form factor at the origin <sup>11</sup>.

In this paper we also assume for simplicity that the mesons are point-like objects, i.e. their interaction with the constituent quarks are described by a local nonderivative Lagrangian. In other words, we choose the effective meson vertex functions to be constant in momentum space. This is a reliable approximation for the light mesons. For heavy mesons we expect that form factor effects in the meson vertex become important. This prevents us from extending the present approach to cases with heavy mesons in the final states, such as  $\Lambda_b^0 \rightarrow \Lambda_c^+ + D_s^-$ . In general the form factor effects in the decays involving heavy mesons in the final state are expected to suppress their rates relative to those obtained from a point-like vertex. Exclusive nonleptonic bottom baryon decays involving heavy mesons form the subject of a separate piece of work.

For the heavy quark propagator  $S_Q$  we will use the leading term in the inverse mass expansion. Suppose  $p = M_{B_Q}v$  is the heavy baryon momentum. We introduce a set the binding energy parameters  $\bar{\Lambda}_{\{q_1q_2\}} = M_{\{Qq_1q_2\}} - m_Q$  which parametrize the difference between the heavy baryon mass  $M_{\{Qq_1q_2\}} \equiv M_{B_Q}$  and the heavy quark mass. Keeping in mind that the vertex function falls off sufficiently fast such that the condition  $|k| \ll m_Q$  holds ( $k$  is the virtual momentum of light quarks) one has

$$S_Q(p+k) = \frac{1}{m_Q - (\not{p} + \not{k})} = S_v(k, \bar{\Lambda}_{\{q_1q_2\}}) + O\left(\frac{1}{m_Q}\right)$$

$$S_v(k, \bar{\Lambda}_{\{q_1q_2\}}) = -\frac{(1 + \not{v})}{2(v \cdot k + \bar{\Lambda}_{\{q_1q_2\}})} \quad (4)$$

In what follows we will assume that  $\bar{\Lambda} \equiv \bar{\Lambda}_{\{uu\}} = \bar{\Lambda}_{\{dd\}} = \bar{\Lambda}_{\{du\}}$ ,  $\bar{\Lambda}_s \equiv \bar{\Lambda}_{\{us\}} = \bar{\Lambda}_{\{ds\}}$ . Thus there are altogether three independent binding energy parameters  $\bar{\Lambda}$ ,  $\bar{\Lambda}_s$ , and  $\bar{\Lambda}_{\{ss\}}$  in our approach.

In the Lagrangian Spectator Model the leptonic coupling constants  $f_\pi$  and  $f_K$  are deter-

mined by the integrals

$$f_\pi = \frac{N_c g_\pi}{4\pi^2} \frac{1}{M_\pi \Lambda^2} \int_{reg} \frac{d^4 k}{\pi^2}, \quad f_K = \frac{N_c g_K}{4\pi^2} \frac{1}{M_K \Lambda \Lambda_s} \int_{reg} \frac{d^4 k}{\pi^2} \quad (5)$$

The meson coupling constants  $g_\pi$  and  $g_K$  in Eq.(5) are determined from *the compositeness condition*<sup>11</sup> which reads

$$1 = \frac{N_c g_\pi^2}{4\pi^2} \frac{1}{M_\pi^2 \Lambda^2} \int_{reg} \frac{d^4 k}{\pi^2}, \quad 1 = \frac{N_c g_K^2}{4\pi^2} \frac{1}{M_K^2 \Lambda \Lambda_s} \int_{reg} \frac{d^4 k}{\pi^2} \quad (6)$$

Equations (5) and (6) contain the ultraviolet divergence since the mesons in our scheme are point-like objects. To regularize these quantities we introduce an ultraviolet cutoff parameter  $\Lambda_{cut} = \Lambda_{q_1} \Lambda_{q_2} / (\Lambda_{q_1} + \Lambda_{q_2})$  with the same  $\Lambda_{q_i}$  as in Eq.(3). Here  $q_i$  corresponds to the flavour of the light quark being the constituent. After that we get

$$f_\pi = \frac{\sqrt{N_c}}{8\pi} \Lambda, \quad f_K = \frac{\sqrt{N_c}}{2\pi} \frac{(\Lambda \Lambda_s)^{3/2}}{(\Lambda + \Lambda_s)^2} \quad (7)$$

Substituting experimental values for  $f_\pi = 131$  MeV and  $f_K = 160$  MeV in Eqs.(7) we obtain  $\Lambda = 1.90$  GeV and  $\Lambda_s = 3.29$  GeV.

Thus, there is the following set of adjustable parameters in our model: the cutoff parameters  $\Lambda_{B_q}$  and  $\Lambda_{B_Q}$ , and the set of binding energy parameters  $\bar{\Lambda}$ ,  $\bar{\Lambda}_s$  and  $\bar{\Lambda}_{\{ss\}}$ .

### 3. Nonleptonic transition matrix elements

The weak nonleptonic decays of bottom and charm baryons are described by the diagrams Fig.1. Diagram I corresponds to the so-called factorizing contribution while the diagrams II and III correspond to the nonfactorizing contributions. \* The vertices  $O_\mu \bullet \bullet O_\mu$  arise from the standard effective four-fermion Lagrangian<sup>15</sup> which for  $b \rightarrow \bar{c}ud$  transitions has the form

$$\mathcal{L}_{\text{eff}} = \frac{G_F}{\sqrt{2}} V_{cb} V_{ud}^\dagger [c_1 (\bar{c}^{a_1} O_\mu b^{a_1}) (\bar{d}^{a_2} O_\mu u^{a_2}) + c_2 (\bar{c}^{a_1} O_\mu b^{a_2}) (\bar{d}^{a_2} O_\mu u^{a_1})] + \text{h.c.} \quad (8)$$

Here  $c_1$  and  $c_2$  are the short distance Wilson coefficients<sup>15</sup>. It is well-known that the factorizing contributions are proportional to the two linear combinations  $a_1 = c_1 + c_2/N_c$  and  $a_2 = c_2 + c_1/N_c$  where  $N_c$  is the number of colours. An analysis of the nonleptonic decays of  $B$  mesons gives the values:  $a_1 \approx 1.05 \pm 0.10$  and  $a_2 \approx 0.25 \pm 0.05$ <sup>15</sup>.

---

\*In the terminology of<sup>5</sup> diagram I corresponds to factorizable external and internal W-emission, IIa to nonfactorizable internal W-emission and IIb and III to nonfactorizable W-exchange.

After some straightforward calculations the matrix element describing exclusive weak nonleptonic decays of bottom baryons can be written as <sup>6 †</sup>

$$M = M_I + M_{IIa} + M_{IIb} + M_{III} \equiv A - \gamma_5 B \quad (9)$$

where the amplitudes  $M_I$ ,  $M_{IIa}$ ,  $M_{IIb}$ , and  $M_{III}$  correspond to the contributions of diagrams I, IIa, IIb, and III in Fig.1, respectively. One has

Factorizing contribution:

$$\text{Diagram I: } M_I = c_W \chi_{\pm} f_P \frac{Q_+}{4M_1 M_2} \left( M_- \ell_{FD}^- - M_+ \ell_{FD}^+ \cdot \gamma^5 \right) f(\omega) \quad (10)$$

Nonfactorizing contributions

$$\text{Diagram IIa: } M_{IIa} = c_W c_- \frac{H_2(\omega)}{4M_1 M_2} \left( P_+ \ell_{IIa}^{P^+} - Q_+ \ell_{IIa}^{Q^+} \cdot \gamma^5 \right) M_1 \quad (11)$$

$$\text{Diagram IIb: } M_{IIb} = c_W c_- \frac{H_2(\omega)}{4M_1 M_2} \left( D_+ \ell_{IIb}^{D^+} - Q_+ \ell_{IIb}^{Q^+} \cdot \gamma^5 \right) M_2 \quad (12)$$

$$\text{Diagram III: } M_{III} = c_W c_- \frac{H_3(\omega)}{4M_1 M_2} \sum_{i=1}^3 M_i (M_1 M_2) \ell_{III} \cdot \gamma^5 \quad (13)$$

Here,  $c_W = (G_F/\sqrt{2})V_{bc}V_{ud}^\dagger$ ;  $\chi_+ = a_1$  for transitions with a charged meson in the final state and  $\chi_- = a_2$  for transitions with a neutral meson in the final state;  $c_- = c_1 - c_2$ , and  $\ell_I^\pm$ ,  $\ell_{IIa}^{P^+}$ ;  $\ell_{IIa}^{Q^+}$ ,  $\ell_{IIb}^{D^+}$ ,  $\ell_{IIb}^{Q^+}$ ,  $\ell_{III}$  are flavor coefficients whose values are listed in Table 1. We employ the notation  $M_{\pm} = M_1 \pm M_2$ ,  $Q_+ = (M_1 + M_2)^2 - M_3^2$ ,  $P_+ = (M_2 + M_3)^2 - M_1^2$ ,  $D_+ = (M_1 + M_3)^2 - M_2^2$ ,  $\omega = (M_1^2 + M_2^2 - M_3^2)/2M_1 M_2$  where  $M_1$ ,  $M_2$  and  $M_3$  are the masses of the initial and final baryons, and the meson, respectively.

The contributions from diagrams IIb and III are down by the helicity suppression factor  $(M_2/M_1)$  relative to the leading diagrams I and IIa in agreement with the results of the spectator model <sup>6</sup>. Note that there are no any additional (dynamical) mass suppression factors for the nonfactorizing diagrams in our approach. In particular there is no mass suppression of diagram IIa. The overlap factors  $f(\omega)$ ,  $H_2(\omega)$  and  $H_3(\omega)$  pertain to the

---

<sup>†</sup>We employ the notation

$$\gamma_5 = \begin{pmatrix} 0 & -I \\ -I & 0 \end{pmatrix}$$

contributions of diagrams I, II and III, respectively and are given by

$$f(\omega) = \frac{R(\omega, \bar{\Lambda})}{R(1, \bar{\Lambda})} \quad (14)$$

$$H_2(\omega) = t_2(r) \frac{R_H(\omega, \bar{\Lambda}^i, \bar{\Lambda}^f)}{\sqrt{R(1, \bar{\Lambda}^i)R(1, \bar{\Lambda}^f)}} \frac{8}{9\pi\sqrt{3}} \frac{\Lambda_{B_Q}^4}{\Lambda^3} \quad (15)$$

$$H_3(\omega) = \frac{1}{2} \exp[9M_3^2/2\Lambda_{B_Q}^2] t_3(r) \frac{R_H(\omega, \bar{\Lambda}^i, \bar{\Lambda}^f)}{\sqrt{R(1, \bar{\Lambda}^i)R(1, \bar{\Lambda}^f)}} \frac{8}{9\pi\sqrt{3}} \frac{\Lambda_{B_Q}^4}{\Lambda^3} \quad (16)$$

where

$$\begin{aligned} R(\omega, \bar{\Lambda}) &= \int_0^\infty duu \int_0^1 d\alpha \exp\left\{-18u^2[1 + 2\alpha(1 - \alpha)(\omega - 1)] + 36u\bar{\Lambda}/\Lambda_{B_Q}\right\} \\ R_H(\omega, \bar{\Lambda}^i, \bar{\Lambda}^f) &= \int_0^\infty duu \int_0^1 d\alpha \exp\left\{-72u^2[1 + 2\alpha(1 - \alpha)(\omega - 1)]\right\} \\ &\quad \times \exp\left\{144u(\bar{\Lambda}^i\alpha + \bar{\Lambda}^f(1 - \alpha))/\Lambda_{B_Q} - 432u^2(\alpha^2 + (1 - \alpha)^2)\right\} \end{aligned}$$

The parameters  $\bar{\Lambda}^i$  and  $\bar{\Lambda}^f$  are the binding energy parameters of the initial and final baryons, respectively. Terms proportional to  $(M_1 - M_2)/\Lambda_{B_Q}$  in the exponents have been dropped for physical reasons. The quantities  $t_i(r)$  ( $r = \Lambda/\Lambda_s$ ) are given by

$$t_2(r) = t_3(r) = (1 + r)^2/4 \text{ for } \Lambda_b^0 \rightarrow \Xi_c^0(\Xi_c'^0) + K^0, \Xi_b^0 \rightarrow \Lambda_c^+(\Sigma_c^+) + K^-,$$

$$t_2(r) = (1 + r)^2/4 \text{ for } \Xi_b^0 \rightarrow \Omega_c^0 + K^0, \Xi_b^- \rightarrow \Sigma_c^0 + K^-,$$

$$t_3(r) = (1 + r)^2/4 \text{ for } \Xi_b^0 \rightarrow \Sigma_c^0 + \bar{K}^0,$$

$$t_2(r) = t_3(r) = r^2/(r^2 \cos^2 \delta_P + \sin^2 \delta_P)^{1/2} \text{ for } \Lambda_b^0 \rightarrow \Sigma_c^0 + \eta,$$

$$t_2(r) = t_3(r) = r^2/(r^2 \sin^2 \delta_P + \cos^2 \delta_P)^{1/2} \text{ for } \Lambda_b^0 \rightarrow \Sigma_c^0 + \eta',$$

$$t_i(r) = r^i/(r^2 \cos^2 \delta_P + \sin^2 \delta_P)^{1/2} \text{ for } \Xi_b^0 \rightarrow \Xi_c^0(\Xi_c'^0) + \eta,$$

$$t_i(r) = r^i/(r^2 \sin^2 \delta_P + \cos^2 \delta_P)^{1/2} \text{ for } \Xi_b^0 \rightarrow \Xi_c^0(\Xi_c'^0) + \eta',$$

and  $t_2(r) = t_3(r) = 1$  for all other modes. We use the notation  $\delta_P = \theta_P - \theta_I$ , where  $\theta_P = -11^\circ$  is the  $\eta - \eta'$  mixing angle,  $\theta_I = 35^\circ$ .

## 4. Results

In this section we give our numerical results for decay rates and asymmetry parameters. The cutoff parameters  $\Lambda_{B_q}$  and  $\Lambda_{B_Q}$ , and the binding energy parameter  $\bar{\Lambda}$  are determined from a fit to known branching ratios of nonleptonic decays  $\Lambda_c^+ \rightarrow \Lambda^0\pi^+$ ,  $\Lambda_c^+ \rightarrow \Sigma^0\pi^+$ ,  $\Lambda_c^+ \rightarrow \Sigma^+\pi^0$ ,  $\Lambda_c^+ \rightarrow p\bar{K}^0$  and  $\Lambda_c^+ \rightarrow \Xi^0 K^+$  (see, Table 2). In the fit we use  $\rho^2 = 1$  for

the slope of the baryonic Isgur-Wise function, leading to  $\Lambda_{B_q} = 3.037$  GeV,  $\Lambda_{B_Q} = 2.408$  GeV,  $\bar{\Lambda} = 0.9$  GeV. The parameters  $\bar{\Lambda}_s$  and  $\bar{\Lambda}_{ss}$  cannot be determined at present due to the lack of experimental information on the decays of heavy-light baryons containing one or two strange quarks. For the time being we fix them at the values  $\bar{\Lambda}_s=1$  GeV and  $\bar{\Lambda}_{ss}=1.1$  GeV. The masses of hadrons are taken from Ref. <sup>1</sup>.

In Table 3 we give our results for the decay rates and asymmetry parameters for the exclusive nonleptonic  $b \rightarrow c\bar{u}s$  decays considered in this paper. A clear pattern emerges. The dominant rates are into channels with factorizing contributions. Rates which proceed only via nonfactorizing diagrams are small but not negligibly small.

In Table 4 we give the contributions of nonfactorizing diagrams relative to those of the factorizing ones for the decay  $\Lambda_b^0 \rightarrow \Lambda_c^+\pi^-$  which we predict to have the largest branching ratio. The values for overlap integrals for this mode are  $f = 0.61$ ,  $H_2=24$  MeV and  $H_3=12$  MeV. The suppressions of the contributions of diagrams IIb and III can in part be traced to the helicity suppression factor. The total contribution of the nonfactorizing diagrams can be seen to be destructive. The sum of nonfactorizing contributions amount up to 30 % of the factorizing contribution in amplitude. Using  $\tau(\Lambda_b) = (1.14 \pm 0.08) \times 10^{-12}$  s <sup>1</sup> we predict a branching ratio of this mode of  $(0.44 \pm 0.003)\%$ . If one neglects the nonfactorizing contributions for this mode as was done in <sup>5</sup> one would obtain an enhanced rate of  $\Gamma = 0.665 \times 10^{10}\text{s}^{-1}$ . The prediction for the asymmetry parameter remains at  $\alpha \simeq -1$  and is thus not affected by such an omission.

In conclusion, we have calculated the exclusive nonleptonic bottom to charm baryon decays  $\frac{1}{2}^+ \rightarrow \frac{1}{2}^+ + 0^-$  with a light pseudoscalar meson in the final state. The dominant rates are into channels with factorizing contributions. Decays which proceed only via the nonfactorizing contributions occur at the 10 % level of the modes with factorizing contributions. In the decay  $\Lambda_b^0 \rightarrow \Lambda_c^+\pi^-$  the total contribution of the nonfactorizing diagrams is destructive and amounts up to 30 % of the factorizing contributions in amplitude. The generalization to the channels  $\frac{1}{2}^+ \rightarrow \frac{1}{2}^+ + 1^-$ ,  $\frac{1}{2}^+ \rightarrow \frac{3}{2}^+ + 0^-$  and  $\frac{1}{2}^+ \rightarrow \frac{1}{2}^+ + 1^-$  involving the ground state partners of the mesons and baryons in the final state is straightforward and will be treated in a subsequent paper. In this paper we discussed only the Cabibbo favoured decays induced by the transitions  $b \rightarrow c\bar{u}d$  with a light meson in the final state. There are also a number of Cabibbo favoured decays with heavy mesons in the final state which include the decays induced by the quark transitions  $b \rightarrow c\bar{c}s$ . The treatment of heavy mesons in the final state requires some refinements in our simple Lagrangian spectator model. Again, exclusive



nonleptonic heavy baryon decays involving heavy mesons in the final state are the subject of a future publication.

### Acknowledgments

M.A.I, V.E.L and A.G.R thank Mainz University for the hospitality where a part of this work was completed. This work was supported in part by the Heisenberg-Landau Program, by the Russian Fund of Fundamental Research (RFFR) under contract 96-02-17435-a, the State Committee of the Russian Federation for Education (project N 95-0-6.3-67, Grant Center at S.-Petersburg State University) and by the BMBF (Germany) under contract 06MZ566. J.G.K. acknowledges partial support by the BMBF (Germany) under contract 06MZ566.

- [1] R.M. Barnett *et al.* Review of Particle Physics, *Phys. Rev.* **D54**, 1 (1996).
- [2] UA1 Collaboration, C. Albajar *et al.*, *Phys. Lett.* **B273**, 540 (1991).
- [3] CDF Collaboration, F. Abe *et al.*, *Phys. Rev.* **D55**, 1142 (1997).
- [4] M. Bauer, B. Stech and M. Wirbel, *Z. Phys.* **C34**, 103 (1987).
- [5] H.-Y. Cheng, *Phys. Rev.* **D56**, 2799 (1997).
- [6] J.G. Körner and M. Krämer, *Z. Phys.* **C55**, 659 (1992).
- [7] J.G. Körner, in *Proc. of the VII International Conference on the Structure of Baryons "Baryons '95"*, eds. P.D. Barnes *et al.* (World Scientific, 1996).
- [8] I.V. Anikin, M.A. Ivanov, N.B. Kulimanova and V.E. Lyubovitskij, *Z. Phys.* **C65**, 681 (1995); *Phys. Atom. Nucl.* **57**, 1021 (1994).
- [9] M.A. Ivanov and V.E. Lyubovitskij, *Phys. Lett.* **B408**, 435 (1997).
- [10] M.A. Ivanov, M.P. Locher, V.E. Lyubovitskij, *Few-Body Syst.* **21**, 131 (1996).
- [11] M.A. Ivanov, V.E. Lyubovitskij, J.G. Körner and P. Kroll, *Phys. Rev.* **D56**, 348 (1997).
- [12] F. Hussain, J.G. Körner and G. Thompson, *Ann. Phys.* **206**, 334 (1991);  
F. Hussain *et al.*, *Nucl. Phys.* **B370**, 259 (1992).
- [13] E.V. Shuryak, *Nucl. Phys.* **B198**, 83 (1982).
- [14] A.G. Grozin and O.I. Yakovlev, *Phys. Lett.* **B285**, 254 (1992).
- [15] A.J. Buras, *Nucl. Phys.* **B434**, 606 (1995).

## List of Tables

**Table 1:** Flavour coefficients for exclusive  $b \rightarrow c\bar{u}d$  nonleptonic heavy baryon decays ( $C \equiv \cos \delta_P$ ,  $S \equiv \sin \delta_P$ ,  $\delta_P = \theta_P - \theta_I$ , where  $\theta_P = -11^\circ$  is the  $\eta - \eta'$  mixing angle,  $\theta_I = 35^\circ$ ).

**Table 2:** Fit of the branchings of nonleptonic decays of charm baryons (in %). Numerical values of CKM elements and Wilson coefficients:  $|V_{cs}| = 0.975$ ,  $|V_{ud}| = 0.975$ ,  $a_1 = 1.3$ ,  $a_2 = -0.65$ .

**Table 3:** Decay rates and asymmetry parameters for exclusive  $b \rightarrow c\bar{u}d$  nonleptonic heavy baryon decays. Numerical values of CKM elements and Wilson coefficients:  $|V_{cb}| = 0.04$ ,  $|V_{ud}| = 0.975$ ,  $a_1 = 1.03$ ,  $a_2 = 0.10$ .

**Table 4:** Decay  $\Lambda_b^0 \rightarrow \Lambda_c^+ \pi^-$ : Contributions of nonfactorizing diagrams relative to contributions of factorizing diagram.

## List of Figures

**Figure 1:** Nonleptonic decay of bottom baryon

Table 1.

| Decay                                       | $\ell_{FD}^-$ | $\ell_{FD}^+$ | $\ell_{II_a}^{P+}$             | $\ell_{II_a}^{Q+}$      | $\ell_{II_b}^{D+}$             | $\ell_{II_b}^{Q+}$             | $\ell_{III}$  |
|---|---------------|---------------|--------------------------------|-------------------------|--------------------------------|--------------------------------|---------------|
| $\Lambda_b^0 \rightarrow \Lambda_c^+ \pi^-$ | -1            | -1            | $-\frac{1}{2}$                 | $\frac{1}{2}$           | $\frac{1}{2}$                  | $\frac{1}{2}$                  | -2            |
| $\Lambda_b^0 \rightarrow \Sigma_c^+ \pi^-$  | 0             | 0             | $\frac{\sqrt{3}}{2}$           | $\frac{1}{2\sqrt{3}}$   | $\frac{\sqrt{3}}{2}$           | $\frac{\sqrt{3}}{2}$           | $-2\sqrt{3}$  |
| $\Lambda_b^0 \rightarrow \Sigma_c^0 \pi^0$  | 0             | 0             | $-\frac{\sqrt{3}}{2}$          | $-\frac{1}{2\sqrt{3}}$  | $-\frac{\sqrt{3}}{2}$          | $-\frac{\sqrt{3}}{2}$          | $2\sqrt{3}$   |
| $\Lambda_b^0 \rightarrow \Sigma_c^0 \eta$   | 0             | 0             | $-\frac{\sqrt{3}}{2}S$         | $-\frac{1}{2\sqrt{3}}S$ | $\frac{\sqrt{3}}{2}S$          | $\frac{\sqrt{3}}{2}S$          | $2\sqrt{3}S$  |
| $\Lambda_b^0 \rightarrow \Sigma_c^0 \eta'$  | 0             | 0             | $\frac{\sqrt{3}}{2}C$          | $\frac{1}{2\sqrt{3}}C$  | $-\frac{\sqrt{3}}{2}C$         | $-\frac{\sqrt{3}}{2}C$         | $-2\sqrt{3}C$ |
| $\Lambda_b^0 \rightarrow \Xi_c^0 K^0$       | 0             | 0             | $\frac{1}{2}$                  | $-\frac{1}{2}$          | 0                              | 0                              | 2             |
| $\Lambda_b^0 \rightarrow \Xi_c'^0 K^0$      | 0             | 0             | $-\frac{\sqrt{3}}{2}$          | $-\frac{1}{2\sqrt{3}}$  | 0                              | 0                              | $2\sqrt{3}$   |
| $\Xi_b^0 \rightarrow \Xi_c^+ \pi^-$         | -1            | -1            | $-\frac{1}{2}$                 | $\frac{1}{2}$           | 0                              | 0                              | 0             |
| $\Xi_b^0 \rightarrow \Xi_c'^+ \pi^-$        | 0             | 0             | $-\frac{\sqrt{3}}{2}$          | $-\frac{1}{2\sqrt{3}}$  | 0                              | 0                              | 0             |
| $\Xi_b^0 \rightarrow \Xi_c^0 \pi^0$         | 0             | 0             | $\frac{1}{2\sqrt{2}}$          | $-\frac{1}{2\sqrt{2}}$  | $\frac{1}{2\sqrt{2}}$          | $\frac{1}{2\sqrt{2}}$          | 0             |
| $\Xi_b^0 \rightarrow \Xi_c^0 \eta$          | 0             | 0             | $\frac{1}{2\sqrt{2}}S$         | $-\frac{1}{2\sqrt{2}}S$ | $-\frac{1}{2\sqrt{2}}S$        | $-\frac{1}{2\sqrt{2}}S$        | $-2C$         |
| $\Xi_b^0 \rightarrow \Xi_c^0 \eta'$         | 0             | 0             | $-\frac{1}{2\sqrt{2}}C$        | $\frac{1}{2\sqrt{2}}C$  | $\frac{1}{2\sqrt{2}}C$         | $\frac{1}{2\sqrt{2}}C$         | $-2S$         |
| $\Xi_b^0 \rightarrow \Xi_c'^0 \pi^0$        | 0             | 0             | $\frac{\sqrt{3}}{2}$           | $\frac{1}{2\sqrt{3}}$   | $\frac{\sqrt{3}}{2}$           | $\frac{\sqrt{3}}{2}$           | 0             |
| $\Xi_b^0 \rightarrow \Xi_c'^0 \eta$         | 0             | 0             | $\frac{\sqrt{3}}{2\sqrt{2}}S$  | $\frac{1}{2\sqrt{6}}S$  | $-\frac{\sqrt{3}}{2\sqrt{2}}S$ | $-\frac{\sqrt{3}}{2\sqrt{2}}S$ | $-2\sqrt{3}C$ |
| $\Xi_b^0 \rightarrow \Xi_c'^0 \eta'$        | 0             | 0             | $-\frac{\sqrt{3}}{2\sqrt{2}}C$ | $-\frac{1}{2\sqrt{6}}C$ | $\frac{\sqrt{3}}{2\sqrt{2}}C$  | $\frac{\sqrt{3}}{2\sqrt{2}}C$  | $-2\sqrt{3}S$ |
| $\Xi_b^0 \rightarrow \Lambda_c^+ K^-$       | 0             | 0             | 0                              | 0                       | $-\frac{1}{2}$                 | $-\frac{1}{2}$                 | 2             |
| $\Xi_b^0 \rightarrow \Sigma_c^+ K^-$        | 0             | 0             | 0                              | 0                       | $-\frac{\sqrt{3}}{2}$          | $-\frac{\sqrt{3}}{2}$          | $2\sqrt{3}$   |
| $\Xi_b^0 \rightarrow \Sigma_c^0 \bar{K}^0$  | 0             | 0             | 0                              | 0                       | 0                              | 0                              | $-2\sqrt{6}$  |
| $\Xi_b^0 \rightarrow \Omega_c^0 K^0$        | 0             | 0             | $\sqrt{\frac{3}{2}}$           | $\frac{1}{\sqrt{6}}$    | 0                              | 0                              | 0             |
| $\Xi_b^- \rightarrow \Xi_c^0 \pi^-$         | -1            | -1            | $\frac{1}{2}$                  | $\frac{1}{2}$           | 0                              | 0                              | 0             |
| $\Xi_b^- \rightarrow \Xi_c'^0 \pi^-$        | 0             | 0             | 0                              | 0                       | $\frac{\sqrt{3}}{2}$           | $\frac{\sqrt{3}}{2}$           | 0             |
| $\Xi_b^- \rightarrow \Sigma_c^0 K^-$        | 0             | 0             | 0                              | 0                       | $-\sqrt{\frac{3}{2}}$          | $-\sqrt{\frac{3}{2}}$          | 0             |
| $\Omega_b^- \rightarrow \Omega_c^0 \pi^-$   | -1            | $\frac{1}{3}$ | 0                              | 0                       | 0                              | 0                              | 0             |

**Table 2.**

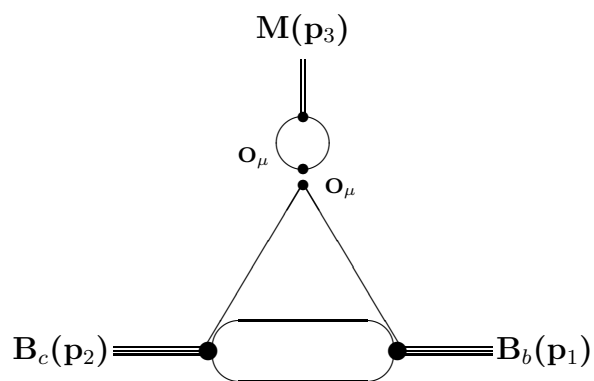
| Process                                 | Our fit | Experiment <sup>1</sup> |
|---|---------|-------------------------|
| $\Lambda_c^+ \rightarrow \Lambda\pi^+$  | 0.79    | $0.79 \pm 0.18$         |
| $\Lambda_c^+ \rightarrow \Sigma^0\pi^+$ | 0.88    | $0.88 \pm 0.20$         |
| $\Lambda_c^+ \rightarrow \Sigma^+\pi^0$ | 0.88    | $0.88 \pm 0.22$         |
| $\Lambda_c^+ \rightarrow p\bar{K}^0$    | 2.06    | $2.2 \pm 0.4$           |
| $\Lambda_c^+ \rightarrow \Xi^0 K^+$     | 0.31    | $0.34 \pm 0.09$         |

**Table 3.**

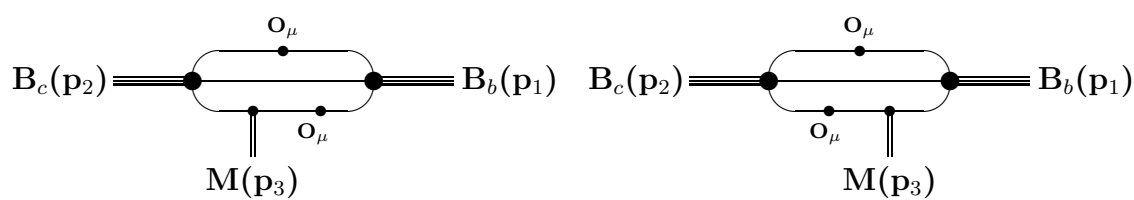
| Process                                    | $\Gamma$ (in $10^{10} \text{ s}^{-1}$ ) | $\alpha$ | Process                                    | $\Gamma$ (in $10^{10} \text{ s}^{-1}$ ) | $\alpha$ |
|--|---|----------|--|---|----------|
| $\Lambda_b^0 \rightarrow \Lambda_c^+\pi^-$ | 0.382                                   | -0.99    | $\Xi_b^0 \rightarrow \Xi_c^0\pi^0$         | 0.014                                   | 0.94     |
| $\Lambda_b^0 \rightarrow \Sigma_c^+\pi^-$  | 0.039                                   | 0.65     | $\Xi_b^0 \rightarrow \Xi_c^0\eta$          | 0.015                                   | -0.98    |
| $\Lambda_b^0 \rightarrow \Sigma_c^0\pi^0$  | 0.039                                   | 0.65     | $\Xi_b^0 \rightarrow \Xi_c^0\eta'$         | 0.021                                   | 0.97     |
| $\Lambda_b^0 \rightarrow \Sigma_c^0\eta$   | 0.023                                   | 0.79     | $\Xi_b^0 \rightarrow \Lambda_c^+K^-$       | 0.010                                   | -0.73    |
| $\Lambda_b^0 \rightarrow \Sigma_c^0\eta'$  | 0.029                                   | 0.99     | $\Xi_b^0 \rightarrow \Sigma_c^+K^-$        | 0.030                                   | -0.74    |
| $\Lambda_b^0 \rightarrow \Xi_c^0 K^0$      | 0.021                                   | -0.81    | $\Xi_b^0 \rightarrow \Sigma_c^0\bar{K}^0$  | 0.021                                   | 0        |
| $\Lambda_b^0 \rightarrow \Xi_c^0 K^0$      | 0.032                                   | 0.98     | $\Xi_b^0 \rightarrow \Omega_c^0 K^0$       | 0.023                                   | 0.65     |
| $\Xi_b^0 \rightarrow \Xi_c^+\pi^-$         | 0.479                                   | -1.00    | $\Xi_b^- \rightarrow \Xi_c^0\pi^-$         | 0.645                                   | -0.97    |
| $\Xi_b^0 \rightarrow \Xi_c^{\prime+}\pi^-$ | 0.018                                   | 0.61     | $\Xi_b^- \rightarrow \Xi_c^{\prime0}\pi^-$ | 0.007                                   | -1.00    |
| $\Xi_b^0 \rightarrow \Xi_c^0\pi^0$         | 0.002                                   | -0.99    | $\Xi_b^- \rightarrow \Sigma_c^0 K^-$       | 0.016                                   | -0.98    |
| $\Xi_b^0 \rightarrow \Xi_c^0\eta$          | 0.012                                   | -0.86    | $\Omega_b^- \rightarrow \Omega_c^0\pi^-$   | 0.352                                   | 0.60     |
| $\Xi_b^0 \rightarrow \Xi_c^0\eta'$         | 0.003                                   | 0.71     |  |   |          |

**Table 4.**

| Amplitude | Diagram |       |           |       |
|-----------|---------|-------|-----------|-------|
|           | IIa     | IIb   | IIa + IIb | III   |
| A         | -13.9%  | -6.2% | -20.1%    |       |
| B         | -14.3%  | -5.8% | -20.1%    | -8.5% |

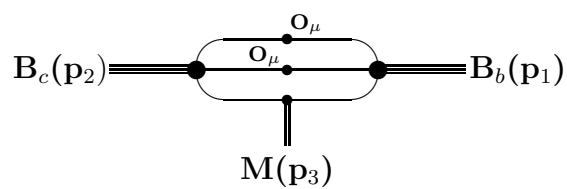


I



IIa

IIb



III

Fig.1